

SEEJPH Volume XXV, 2024, ISSN: 2197-5248; Posted:12-12-2024

# Molecular Docking Studies and In silico ADMET analysis of 1, 4 disubstituted, 1, 2, 3 Triazole Derivatives as Hemagglutinin and Neuraminidase inhibitors for Antiviral Activity against H1N1 **Influenza Virus**

## Pavankumar D Chopade\*, Anwar Rafique Shaikh

Department of Pharmachemistry, M. C. E. Society's Allana College of Pharmacy, Azam Campus, Camp, Pune-411001, Maharashtra, India.

\*Corresponding author Pavankumar D. Chopade,

Research Scholar

#### Address:

Department of Pharmachemistry, M. C. E. Society's Allana College Of Pharmacy, Azam Campus, Camp. Pune-411001, Maharashtra, India.

#### **E-mail:** chopadepavan@gmail.com **KEYWORDS ABSTRACT**

1, 2, 3 Triazoles, Synthesis, virus, Antiviral activity.

1,2,3-triazole is a basic aromatic heterocyclic scaffold that is used in a variety of drug discovery applications, including anticancer, anti-Alkynes, Azides, inflammatory, antiviral, anti-convulsant, anti-tubercular, antimicrobial, and (H1N1) influenza antidiabetic. 1, 4 Disubstituted 1,2,3-triazoles can be produced by the azide alkyne Huisgen's cycloaddition, which involves an azide and an alkyne undergoing a 1,3-dipolar cycloaddition reaction. A 1,2,3-triazoles and their derivatives can be synthesized using a variety of metal catalysts (including Cu, Au, Ag, Zn, Sm, Ni, Ru, Ir, Rh, and Pd,), organ catalysts, solvent-free and catalyst-free neat syntheses as well as solvent- and catalyst-free neat syntheses. Ongoing developments suggest that 1,2,3-triazoles will contribute to future organic synthesis and are useful for the creation of molecular libraries of various functionalized 1,2,3-triazoles. This research paper primarily emphasizes the design and docking of several derivatives that exhibit notable antiviral efficacy against the H1N1 influenza virus, novel methods for drug design, and their corresponding drug targets. It aims to present various strategies for creating new drug entities. complemented by docking studies, to assist emerging researchers in exploring fresh dimensions of molecules.

## INTRODUCTION

1,2,3-Triazole is an aromatic, unsaturated, five-membered nitrogen-containing heterocycle with a 6p electron framework, consisting of three standard nitrogen atoms and two carbon atoms featuring two double bonds. Every atom in 1,2,3-triazoles is sp2 hybridized, and the available 6p electrons are delocalized throughout the ring, which contributes to its aromatic properties.. 1,2,3-Triazoles are primarily divided into three categories: (1) monocyclic 1,2,3-triazoles, (2) benzotriazoles, and (3) 1,2,3-triazolium salts. The monocyclic 1,2,3-triazoles are further subdivided into three subclasses based on the location of the NH proton. The 1H- and 2H-1,2,3-triazoles exist in an equilibrium state both in solution and in the gaseous phase and exhibit aromatic properties, whereas 4H-1,2,3-triazole is classified as nonaromatic. The advancement of synthetic approaches



SEEJPH Volume XXV, 2024, ISSN: 2197-5248; Posted:12-12-2024

for producing triazoles and their derivatives is crucial, as 1,2,3-triazoles, in particular, are solely of synthetic origin; it poses significant challenges for biological mechanisms to synthesize compounds with three adjacent nitrogen atoms in a five-membered cyclic structure. This versatile scaffold exhibits significant therapeutic potential, including antiallergic, antimalarial, antiviral, antimicrobial, antitumor, antifungal, antiparasitic, antioxidant, anti-³inflammatory, anticonvulsant, anthelmintic, anti-HIV, CNS depressant, and analgesic properties.<sup>4</sup> Due to their broad spectrum of pharmacological activities, 1,2,3-triazoles and their derivatives continue to be extensively researched for the development of novel and effective drugs. The synthesis of 1,2,3-triazole has undergone remarkable advancements, primarily driven by the adaptability of CuAAC (coppercatalyzed azide-alkyne cycloaddition), a key reaction in azide—alkyne addition. <sup>5</sup>

## Molecular Docking and drug design

The primary objective of molecular docking is to computationally predict the structure of a ligand-receptor complex. This process involves two interconnected steps: first, generating various conformations of the ligand within the protein's active site, and then evaluating and ranking these conformations using a scoring function. Ideally, the sampling algorithms should accurately replicate the experimentally observed binding mode, while the scoring function should prioritize it as the highest-ranked conformation. With these key aspects in mind, we provide a concise overview of fundamental docking principles. <sup>6</sup>

AutoDock employs a computationally efficient "hybrid" force field that integrates molecular mechanics-based terms with empirical components. While its prediction of absolute binding energies may be less precise than more computationally demanding, purely force field-based methods, this semi-empirical approach is well-suited for relative ranking. The AutoDock force field incorporates intramolecular interactions, a comprehensive desolvation model, and accounts for hydrogen bond directionality. Conformational entropy is determined by summing the torsional degrees of freedom. Although water molecules are not explicitly modeled, pairwise atomic terms estimate their contributions, including dispersion/repulsion, hydrogen bonding, electrostatics, and desolvation, with calibration weights derived from experimental data. The evaluation process consists of two main steps: first, computing the energy of the ligand and protein in their unbound states, and second, determining the energy of the protein-ligand complex. Then take the difference between 1 and 2.

$$\begin{split} \Delta G &= (V_{\text{bound}}^{\text{L-L}} - V_{\text{unbound}}^{\text{L-L}}) + (V_{\text{bound}}^{\text{P-P}} - V_{\text{unbound}}^{\text{P-P}}) \\ &+ (V_{\text{bound}}^{\text{P-L}} - V_{\text{unbound}}^{\text{P-L}} + \Delta S_{\text{conf}}) \end{split}$$

Where P refers to the protein, L refers to the ligand, V are the pair-wise evaluations mentioned above, and  $\Delta S\sim conf\sim$  denotes the loss of conformational entropy upon binding (R Huey et al., 2016).<sup>7</sup>

Binding energy quantifies the affinity between a ligand and a protein complex, representing the difference between the energy of the bound complex and the sum of the energies of the individual molecules. Ligand efficiency is defined as the binding energy per ligand atom interacting with the protein. Intermolecular energy refers to the energy between non-bonded atoms, including interactions between atoms separated by 3–4 bonds or those in different molecules. Desolvation energy accounts for the loss of electrostatic and/or van der Waals interactions between the ligand or protein and the



SEEJPH Volume XXV, 2024, ISSN: 2197-5248; Posted:12-12-2024

solvent upon binding. Electrostatic energy represents non-bonded interactions and differs from electrostatic desolvation energy, as it reflects changes in the electrostatic energy of the ligand or protein upon binding. Total energy encompasses the sum of all energetic changes in the ligand or protein upon binding, including those captured by the scoring function, along with entropic contributions. Torsion energy relates to the dihedral component of internal energy.<sup>8</sup>

The inhibition constant (Ki) measures the potency of an inhibitor, representing the concentration needed to achieve half-maximal inhibition. The electrostatic potential surrounding each docked molecule is determined by solving the linearized Poisson-Boltzmann equation using the finite-difference method, as implemented in the Delphi program (Klapper et al., 1986; Honig & Nicholls, 1995). These calculations are carried out on a fine grid with a resolution of 0.5 Å, ensuring precise potential estimations. The potential calculation is independent of the docking process, which is executed by a program MolFit. MolFit reads the precomputed potential files for both molecules, along with data on the grid interval and the potential grid's origin. Consequently, electrostatic potentials calculated using alternative programs or different force field parameters can be incorporated to characterize the electrostatic properties of the docked molecules.<sup>9</sup>

#### Materials and methods

Hemagglutinin is glycoproteins involved in receptor binding and membrane fusion, produced by viruses in the Paramyxoviridae family. These proteins facilitate viral attachment and infection by binding to receptors on red blood cells. The process of red cell agglutination occurs when antibodies on one cell interact with those on another, leading to the formation of irregular clumps. Hemagglutinin specifically recognizes glycoconjugates on the surface of host red blood cells that contain sialic acid, albeit with low affinity, and utilize them to gain entry into the host cell's endosome. Once inside the endosome, hemagglutinin undergoes conformational changes at an acidic pH of 5–6.5, activating a fusion peptide that enables viral attachment. The phenomenon of agglutination and the role of hemagglutinin were first identified by virologist George K. Hirst in 1941. Later, in 1957, Alfred Gottschalk demonstrated that hemagglutinin mediate viral binding to host cells by attaching to sialic acids present on the carbohydrate side chains of cell-membrane glycoproteins and glycolipids. <sup>10</sup>

Neuraminidase enzymes form a diverse family found across various organisms. The most well-known among them is viral neuraminidase, which serves as a key target for antiviral drugs aimed at preventing the spread of influenza. Viral neuraminidases often act as antigenic markers on the surface of the influenza virus, with certain variants contributing to increased virulence. In addition to their viral forms, homologous neuraminidases are present in mammalian cells, where they perform a range of biological functions. The human genome encodes at least four mammalian sialidase homologues (NEU1, NEU2, NEU3, and NEU4). Sialidases, also known as neuraminidases, can function as pathogenic factors in microbial infections. These enzymes catalyze the cleavage of terminal sialic acid residues from both newly formed virions and host cell receptors. Their activity plays a crucial role in facilitating viral movement through respiratory tract mucus and aiding in the release of progeny virions from infected cells.<sup>11</sup>

#### **Selection of Ligands:**

Several ligands were obtained from the PubChem drug database and docked against Hemagglutinin (3AL4) and Neuraminidase (4B7Q) using AutoDock V4.2 software. The ligands, labeled A1 to A14, were selected based on a comprehensive literature review of existing ligands for these proteins. A total of 10 previously identified ligands were chosen to enhance understanding and insights in the current study. 12



SEEJPH Volume XXV, 2024, ISSN: 2197-5248; Posted:12-12-2024

### **Ligand Preparation-**

The 3D structures of the inhibitors, along with their corresponding PubChem CIDs, were retrieved and saved in SDF format. Subsequently, ligand preparation involved processing these 3D structures in PyMOL software, where they were converted from SDF to PDB format. Additionally, any metal components present in the ligand structures were removed using PyMOL to ensure suitability for docking studies.<sup>13</sup> The finalized ligands were then saved in PDB format for further docking analysis.

## Protein preparation-

The crystal structures of the target proteins were obtained from the Protein Data Bank (PDB) and used for further analysis in the docking process.<sup>14</sup>

- 1. PDB ID: 3AL4, Protein name: Hemagglutinin, Organism(s): Influenza A virus (A/California/04/2009(H1N1), Resolution: 2.87Å, Sequence Length=333, Uniprot ID C3W5S1, Gene Names: Hemagglutinin, HA.
- 2. PDB ID: 4B7Q, Protein name: Neuraminidase, Organism(s): Influenza A virus (A/California/04/2009(H1N1), Resolution: 2.73Å, Sequence Length=469, Uniprot ID C7FH46, Gene Names: NA.

## **Molecular docking Operation**

Molecular docking plays a crucial role in computer-assisted drug discovery by predicting the intermolecular interactions between a protein and ligand, providing insights into their binding affinity. Docking simulations were conducted using the AutoDock 4.2.6 program, which utilizes an empirical free energy function and the Lamarckian Genetic Algorithm (LGA). The grid maps for the docking process were generated using AutoGrid, with a grid size of 48 x 40 x 68 points and a grid-point spacing of 1.000 Å. The best docking conformation, which exhibited the lowest binding energy, was selected from the search results. The protein-ligand interaction, including hydrogen bonds and bond lengths, was analyzed using PyMOL, UCSF Chimera, and Accelrys Discovery Studio Visualizer software.<sup>15</sup>

## **Result and Discussion**

On performing the docking of the Hemagglutinin(3AL4) with A1(-5.40kcal/mol), A2(-5.49kcal/mol), A4(-4.34kcal/mol), A6(-5.05kcal/mol), A8(-4.72kcal/mol), A9(-6.44kcal/mol), A11(-4.87kcal/mol), A12(-4.96kcal/mol), A13(-6.13kcal/mol) and A14(-5.29kcal/mol) it was observed that the binding energy shown by the protein and ligand is good for all the compounds and best at A9(-6.44kcal/mol). On performing the docking of the Protein name the Protein Neuraminidase (4B7Q) with A1(-4.74kcal/mol), A2 (-6.03kcal/mol), A4(-4.55kcal/mol), A6(-4.65kcal/mol), A8(-4.37kcal/mol), A9 (-5.09kcalmol), A11(-4.60kcal/mol), A12(-4.24kcal/mol), A13(-5.62kcal/mol) and A14 (-4.60kcal/mol) at it was observed that the binding energy shown by the protein and ligand is good for all the compounds and best at A2 (-6.03kcal/mol)

Number of torsions are choosen from 0-6, and if any ligand shows more than 6 it is adjusted to 6. Hydrogen bond interactions are also calculated and mentioned, presence of H-bonds depicts stable interaction between ligand and protein. Discovery studio 2020 Client and Chimera softwares are used to depict Hydrogen bonds, 2-D images and protein-ligand interactions images for a good visualization of the docking.

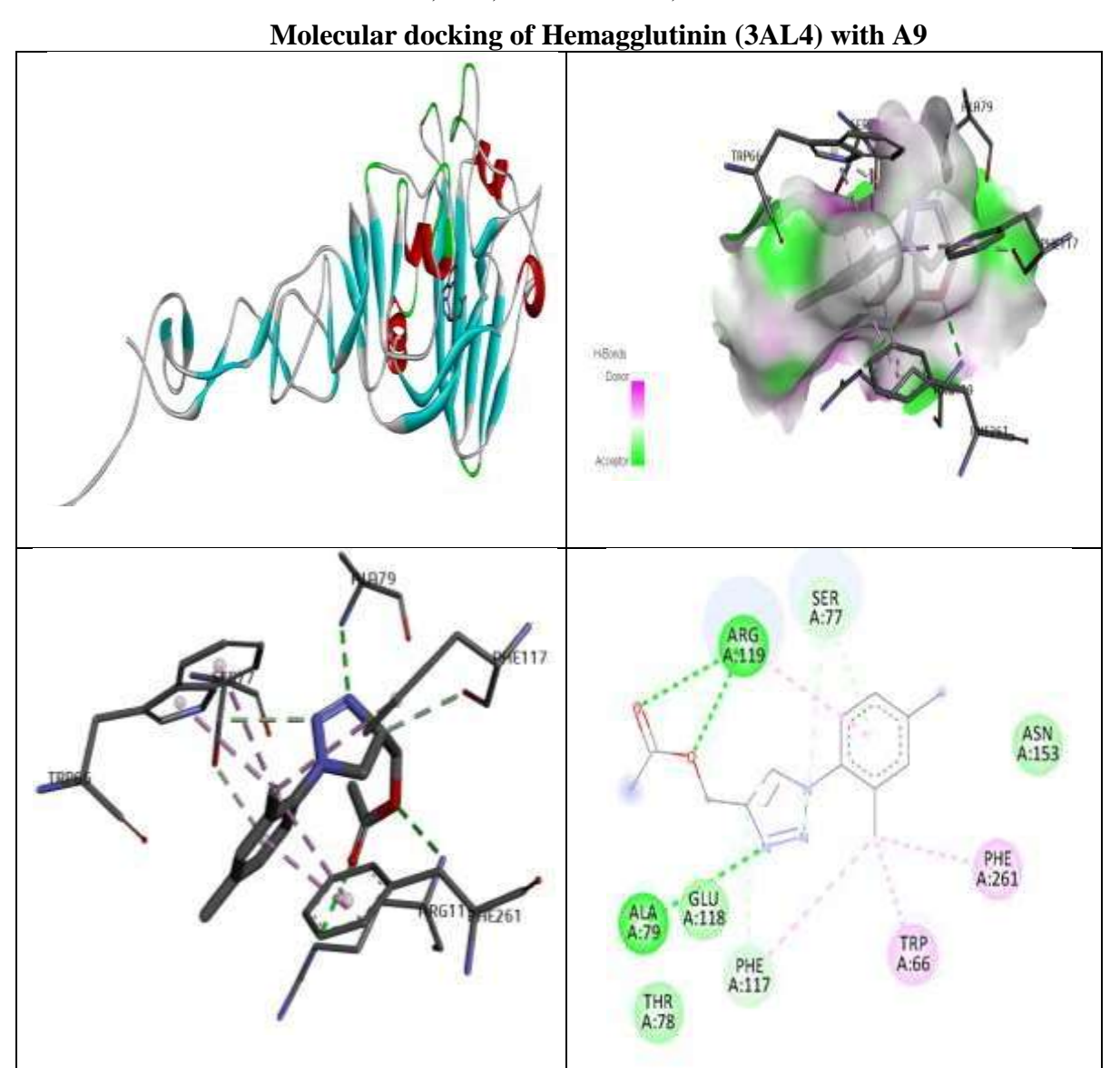


Table1: Docking results of the Hemagglutinin (3AL4) with A1-A14								
Protein s Name	Ligand Name	Binding Energy (kcal/mo	No. of H Bonds	Interacting residue	Final Intermole cular Energy (kcal/mol)	vdW + Hbond + desolv Energy (kcal/mol)	Electrosta tic Energy (kcal/mol)	Torsional Free Energy (kcal/mol)
	A1	-5.40	02 H1:3.33Å H2:3.14Å	ALA:79(H1), ARG:119(H2) , TRP:66, SER:77, PHE:117.	-6.27	-6.06	-0.22	+1.19
	A2	-5.49	01 H1:2.89Å	ARG:51(H1), LEU:50, GLY:307, SER:83, SER:269.	-6.91	-5.75	-1.16	+1.49
	A4	-4.34	02 H1:2.16Å H2:3.16Å	THR:305(H1), ARG:108(H2)	-5.63	-5.22	-0.41	+1.49
3AL4	A6	-5.05	02 H1:2.63Å H2:3.00Å	TRP:66(H1), ARG:119(H2) , SER:77, THR:78.	-6.06	-5.85	-0.21	+1.49
	A8	-4.72	00	PRO:55, LEU:76, VAL:278.	-5.50	-5.47	-0.04	+1.19
	A9	-6.44	02 H1:3.31Å H2: 3.16Å	ALA:79(H1), ARG:119(H2) , SER:77, PHE:117, TRP:66, PHE:261	-7.20	-6.95	-0.25	+1.19
	A11	-4.87	04 H1:2.28Å H2:1.96Å H3:2.61Å H4:2.86Å	ALA:54(H1), SER:81(H2), THR:78(H3), HIS:57(H4), ALA:79.	-6.06	-6.03	-0.03	+1.79
	A12	-4.96	04 H1:2.83Ă H2:3.27Ă H3:1.17Ă H4:3.16 Å	SER:149(H1), PHE:150(H2), LYS:152(H3), LYS:125(H4).	-5.93	-5.40	-0.53	+1.49
	A13	-6.13	03 H1:2.75Å H2:3.03Å H3:2.85Å	ARG:51(H1), LYS:308(H2), GLY:307(H3).	-7.91	-4.87	-3.04	+1.79
	A14	-5.29	02 H1:2.21Å H2:3.03Å	SER:81(H1), HIS:57(H2), ALA:54, ALA:79, LEU:56.	-5.42	-5.37	-0.05	+1.79



Table 2: Docking results of the Neuraminidase (4B7Q) with A1-A10.								
Protei ns Name	Ligand Name	Bindi ng Energ y (kcal/ mol)	No. of H Bonds	Interacting residue	Final Intermol ecular Energy (kcal/mo l)	vdW + Hbond + desolv Energy (kcal/mo l)	Electros tatic Energy (kcal/mo l)	Torsion al Free Energy (kcal/mo l)
	A1	-4.74	03 H1:2.63Å H2:3.13Å H3:2.86Å	ARG:293(H1), ARG:368(H2), TYR:402(H3), ARG:225, ARG:152.	-5.78	-5.21	-0.57	+1.19
	A2	-6.03	04 H1:2.46Å H2:3.14Å H3:2.88Å H4:2.79Å	LYS:432(H1), ARG:368(H2), TYR:402(H3), ARG:293(H4), PRO:326.	-7.36	-4.62	-2.73	+1.49
	A4	-4.55	04 H1:3.08Å H2:2.81Å H3:2.32Å H4:3.00Å	ARG:293(H1), ARG:368(H2), SER:366(H3), GLY:345(H4), PRO:326.	-5.77	-5.27	-0.50	+1.49
	A6	-4.65	05 H1:2.52Å H2:2.26Å H3:3.00Å H4:3.11Å H5:3.39Å	ASN:325(H1), SER:366(H2), GLY:345(H3), ARG:293(H4), ARG:368(H5), PRO:326.	-6.01	-5.52	-0.49	+1.49
	A8	-4.37	03 H1:2.94Å H2:2.90Å H3:2.94Å	ARG:293(H1), ARG:368(H2), GLY:345(H3), PRO:326.	-5.27	-4.86	-0.41	+1.19
4B7Q	A9	-5.09	03 H1:2.98Å H2:3.33Å H3:3.10Å	TYR:402(H1), ARG:293(H2), ARG:368(H3), PRO:431, ASP:151, LYS:432, ILE:427.	-6.20	-5.57	-0.63	+1.19
	A11	-4.60	06 H1:3.14Å H2:2.11Å H3:2.55Å H4:2.43Å H5:3.31Å H6:2.17Å	ARG:293(H1), TRP:179(H2), GLU:278(H3), SER:180(H4), ARG:152(H5), GLU:228(H6), ARG:225, ILE:223.	-5.91	-5.56	-0.35	+1.79
	A12	-4.24	04 H1:3.05Å H2:3.19Å H3:3.20Å H4:2.78Å	LYS:432(H1), GLY:345(H2), ARG:293(H3), ARG:368(H4), SER:366, PRO:326.	-5.44	-4.91	-0.52	+1.49
	A13	-5.62	03 H1:3.23Å H2:3.11Å H3:3.03Å	GLY:345(H1), ARG:293(H2), ARG:368(H3).	-7.21	-4.95	-2.26	+1.79
	A14	-4.60	02 H1:2.12Å H2:3.30Å	SER:176(H1), VAL:177(H2), VAL:205.	-4.68	-4.58	-0.10	+1.79





**Figure 6**. Molecular docking of **Hemagglutinin** (3AL4)Binding Domain Complexed with A9 shows 3D model of the interactions and the 2D interaction patterns and H-bond interaction.



SEEJPH Volume XXV, 2024, ISSN: 2197-5248; Posted:12-12-2024

## Molecular docking of Neuraminidase (4B7Q) with A2

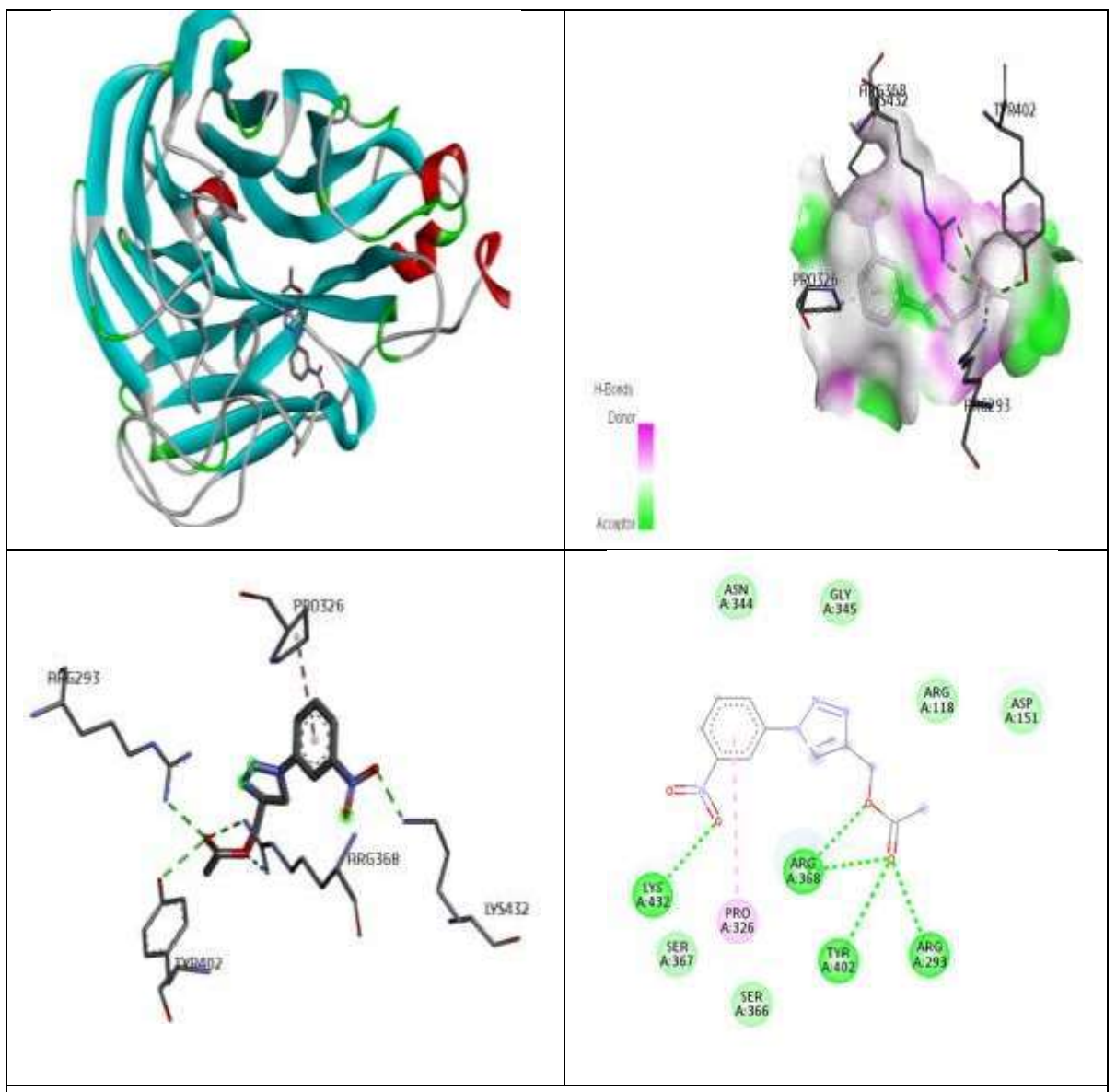


**Figure 2**. Molecular docking of **Neuraminidase** (**4B7Q**) Binding Domain Complexed with **A2** shows 3D model of the interactions and the 2D interaction patterns and H-bond interaction.

## ADMET ANALYSIS TEST REPORT

Chemical absorption, distribution, metabolism, excretion, and toxicity (ADMET) are essential factors in drug discovery and development. An effective drug candidate must not only demonstrate sufficient efficacy against its therapeutic target but also possess favorable ADMET properties at therapeutic doses. A successful drug requires a well-balanced combination of biochemical activity, pharmacokinetics, and safety. Along with high potency and selectivity, a favorable ADMET profile is equally important for the success of a drug



SEEJPH Volume XXV, 2024, ISSN: 2197-5248; Posted:12-12-2024

candidate. 17

#### **SOFTWARES USED:**

here are several software tools available to predict ADMET properties. In this study, we used ADMETlab 2.0 (https://admetmesh.scbdd.com/) for ADMET property predictions. ADMETlab 2.0 was developed using the Django Python web framework and deployed on an elastic compute service from Aliyun, operating on an Ubuntu Linux system. Web access was facilitated through the Nginx web server, and the interactions between Django and the proxy server were managed by uwsgi. The application was built using the Model-View-Template (MVT) framework. The model layer connects business objects to database objects. The view layer serves as the business logic layer, handling access to deep learning models, delivering data to the template layer for display, and managing file uploads and downloads. The template layer is responsible for visualizing results, rendering pages, and integrating documentation. Uploaded and downloaded files, pre-trained models, and model predictions are stored on the server. On the server.

Key ADMET properties, along with those covered under Lipinski's Rule of Five (RO5), including molecular weight, hydrogen bond donors/acceptors, and the octanol/water partition coefficient (QPlogPo/w), were predicted using QikProp, a module within the Schrödinger software suite. <sup>23-24</sup>

## **ADMET STUDIES:**

Computational ADMET prediction (absorption, distribution, metabolism, excretion, and toxicity) is a fundamental approach in modern drug discovery to assess the pharmacokinetics and toxicity of potential drugs. These properties are crucial for selecting and developing drug candidates. The ADMET properties of compounds A1 to A14 were evaluated using ADMETlab. A higher Human Intestinal Absorption (HIA) indicates that a compound is likely to be better absorbed when taken orally. The compound with the best Blood Brain Barrier (BBB) penetration emerged as the top drug candidate. Additionally, assessing the toxicity of chemical compounds is essential to determine their potential harmful effects on humans, animals, plants, or the environment..<sup>26</sup> There are various other properties which are listed below:

Table: Performance of the classification models incorporated into the ADMET lab 2.0 platform for Compound **A2** 

Category	Model	Points
Absorption	Caco-2 Permeability	-4.734
	MDCKPermeability	0.00026
	TheMadin-Darby	
	canine kidney:	
	Pgp-	
	inhibitor(Permeability	
	glycoprotein)	
	Pgpsubstrate(permeability	
	glycoprotein)	
	HIA (Human Intestinal	
	Absorption)	
Distribution	PPB(Plasma protein	93.746%
	binding)	
	VD(Volume Distribution)	1.020
	BBB Penetration(Blood	-
	Brain Barrier)	
	Fu	10.225%



N/1-4-11:	CVD1 A 21 - 1-11-14 - 11	
Metabolism	CYP1A2inhibitor	+++
	(Cytochrome P4501)	
	CYP1A2 substrate	
	CYP2C19	++
	inhibitor(Cytochrome	
	P4502)	
	CYP2C19 substrate	-
	CYP2C9	_
	inhibitor(Cytochrome	
	P450 family 2 subfamily	
	C member 9)	
	CYP2C9 substrate	+
	CYP2D6	
	inhibitor(Cytochrome	
	P450 2D6)	
	CYP2D6 substrate	+
	CYP3A4	
	inhibitor(Cytochrome	
	P450 3A4)	
	CYP3A4 substrate	+
T4°		
Excretion CL		1.973
	T1/2(half life of the	0.785
	reaction)	
Toxicity	hERG Blockers (Human	-
	ether à-go-go related	
	gene)	
	H-HT	++
	DILI	++
		+++
		++
	FDAMDD	+
	Skin Sensitization	+++
	Carcinogencity	+++
	Respiratory Toxicity	++
	Bioconcentration Factors	0.493
	IGC50(Inhibition Growth	4.388
	concentration)	
	LC50FM(Lethal Dose)	4.538
	LC50DM	4.752
Physicochomical	Molecular Weight (MW)	246.090
Physicochemical Property	Molecular weight (MW)	2 <del>4</del> 0.070
Property	Volume	245 020
	Volume	245.029
	Density	1.078
	nHA(No of hydrogen	8
acceptor)		
	nHD(No of hydrogen	0
	donor)	
	nRot(No of rotatable	5
	1 2 1 2 1 2 1 2 1 2 1 2 1 2 1 2 1 2 1 2	<u>l</u>



SEEJPH Volume XXV, 2024, ISSN: 2197-5248; Posted:12-12-2024

bonds)	
nRing(No of rings)	2
MaxRing(Maximum no	6
of rings)	
nHet(No of heteroatoms)	8
fChar(Formal charge)	0
nRig (No of rigid bonds)	13
Flexibility	0.385
Stereo Centers	1
TPSA(Topological polar	97.400
surface area)	
logS(Measuring	-4.038
solubility)	
logP(Measuring	-2.934
lipophliicity)	
logD(Distribution	2.933
Coefficient)	

## Lipinski rule of 5 information for synthesized compounds -

Sr. No.	Name of Co- former	Mol Weight (g/mol)	XLogP3	Hydrogen Bond Donor	Hydrogen Bond Acceptor	Molar Refractivity
1	A1	217.000000	1.805500	0	5	59.064991
2	A2	262.000000	1.713700	0	7	65.719398
3	A4	233.000000	1.511100	1	6	60.729794
4	A6	232.000000	1.387700	2	6	63.477390
5	A8	231.000000	2.113920	0	5	63.801991
6	A9	245.000000	2.422340	0	5	68.538994
7	A11	247.000000	0.183600	4	7	64.606796
8	A12	247.000000	1.814100	0	6	65.616989
9	A13	307.000000	1.621900	0	9	72.373795
10	A14	249.000000	1.216700	2	7	62.394596

#### **Conclusion**

Our study concludes that ester-linked 1,4-disubstituted 1,2,3-triazoles derivatives is inhibiting hemagglutinin (HA), neuraminidase (NA) with high binding affinity. The strength of binding affinity and the interaction at the site of inhibition reveals that it is a good source of synthetic remedy. Further experimental studies required to check efficacy of these agent for the treatment. The Superfluity research comprehends and explained great diversity of an antiviral agents. This Study gives clue about the further modification in the main nucleus may provide potent therapeutic application toward the H1N1 Swine Flu Influenza Virus Infection. We can substitute 1,2,3-triazoles with different aromatic and heterocyclic groups and go for further molecular docking study with respective target. The findings of this investigation indicate that compounds A1-A14 suppress the proliferation and infection of the influenza A virus in MDCK cells. This finding offers crucial information on the structures of substances that can be employed to create influenza medications that target the host cell's hemagglutinin (3AL4) and neuraminidase (4B7Q) proteins. As a result, these findings contribute to establish the chemical structures of compounds that could be used in developing influenza medicines. The docking investigations showed that the reported compounds have quite good binding affinities (-4.37 to -6.44 kcal/mol) with the proteins. There is potential for the reported



SEEJPH Volume XXV, 2024, ISSN: 2197-5248; Posted:12-12-2024

compounds to be utilized as antiviral medications in the future. Nevertheless, further research needs to be conducted to discover the full potential of these compounds as an antiviral agent, apparently offering fresh opportunities for fighting influenza and other viral infections.

#### **Declarations:**

Ethics approval and consent to participate- Not applicable.

**Consent for publication-** The authors declares no completing financial interest.

Availability of data and material- Data and materials are available upon request.

**Competing interests**- There are no competing interests to declare for all authors.

**Funding-**The author declare that no funds, authorship and other support received from anyone.

**Conflicts of interest:** The authors declare that there is no conflict of interest.

**Acknowledgements-** The authors are thankful to the SPPU, Pune and MCE'S Allana College of Pharmacy, Pune for extending their support in whole research work. **References:** 

- 1. Kumar, S.; Khokra, S.L.; Yadav, A. Triazole Analogues as Potential Pharmacological Agents: A Brief Review. Futurure J. Pharm. Sci. 2021, 7 (1), 106. doi:10.1186/s43094-021-00241-3..
- 2. Nehra, N.; Tittal, R.K.; Ghule, V.D. 1, 2, 3-Triazoles of 8-Hydroxyquinoline and HBT: Synthesis and Studies (DNA Binding, Antimicrobial, Molecular Docking, ADME, and DFT). ACS Omega 2021, 6, 27089–27100. doi:10.1021/acsomega.1c03668
- 3. W. Peng and S. Zhu, "Efficient Synthesis of 5-Fluoroalkylated 1H-1,2,3-Triazoles and Application of the Bromodifluoromethylated Triazole to the Synthesis of Novel Bicyclic Gem-difluorinated 1H-pyrano[3,4-d][1,2,3]-triazol-4-one Compounds," Tetrahedron 59, no. 24 (2003): 4395–04.
- 4. PavanKumar D. Chopade\* and Anwar Rafique Shaikh, "advancements and future perspectives of 1, 2, 3 triazole scaffold as promising antiviral agent in drug discovery", IJPSR (2022), Volume 13, Issue 12, 4805-4818
- 5. Wahab, A.; Gao, Z.; Gou, J.; Yu, B. The Construction of Phosphonate Triazolyl by Copper (II)-Catalyzed Furan Dearomatized [3+2] Cycloaddition. Org. Biomol. Chem. 2022, 20, 6319–6323.
- 6. Sowmya, H., & Setti Sudharshan, M. (2023, March 6). Molecular modeling and docking analysis of Swine flu (H1N1) Neuraminidase protein against the phytochemicals of andrographis paniculata. Journal of microbiology, biotechnology and food sciences, e4751. https://doi.org/10.55251/jmbfs.4751
- 7. Bogoyavlenskiy, A., Zaitseva, I., Alexyuk, P., Alexyuk, M., Omirtaeva, E., Manakbayeva, A., Moldakhanov, Y., Anarkulova, E., Imangazy, A., Berezin, V.,
  - Korulkin, D., Hasan, A. H., Noamaan, M., & Jamalis, J. (2023, December 8). Naturally Occurring Isorhamnetin Glycosides as Potential Agents against Influenza Viruses: Antiviral and Molecular Docking Studies. ACS Omega, 8(50), 48499–48514. https://doi.org/10.1021/acsomega.3c08407
- 8. Shi, Y., Zhang, X., Yang, Y., Cai, T., Peng, C., Wu, L., Zhou, L., Han, J., Ma, M., Zhu, W., & Xu, Z. (2023, September). D3CARP: a comprehensive platform with



- multiple-conformation based docking, ligand similarity search and deep learning approaches for target prediction and virtual screening. Computers in Biology and Medicine, 164, 107283. https://doi.org/10.1016/j.compbiomed.2023.107283
- 9. Yildirim, M., & Celik, I. (2024, April 29). Applications of Molecular Docking Studies in SARS-CoV-2 Targeted Drug Discovery and the Gains Achieved through Molecular Docking. Unravelling Molecular Docking From Theory to Practice [Working Title]. https://doi.org/10.5772/intechopen.1004804
- 10. Mehrbod P, Abdalla MA, Fotouhi F, Heidarzadeh M, Aro AO, Eloff JN, McGaw LJ, Fasina FO. Immunomodulatory properties of quercetin-3-O-α-L-rhamnopyranoside from Rapanea melanophloeos against influenza a virus. BMC Complement Altern Med. 2018;18:1–10.
- 11. Shigeta S, Mori S, Watanabe J, Soeda S, Takahashi K, Yamase T. Synergistic antiinfluenza virus A (H1N1) activities of PM-523 (polyoxometalate) and Ribavirin in vitro and in vivo. Antimicrob Agents Chemother. 1997;41:1423–7.
- 12. Trott, O. & Olson, A.J. AutoDock Vina: improving the speed and accuracy of docking with a new scoring function, efficient optimization, and multithreading. J. Comput. Chem. 31, 455–461 (2010).
- 13. Morris, G.M. et al. Automated docking using a Lamarckian genetic algorithm and an empirical binding free energy function. J. Comput. Chem. 19, 1639–1662 (1998).
- 14. Morris, G.M. et al. AutoDock4 and AutoDockTools4: automated docking with selective receptor flexibility. *J. Comput. Chem.* **30**, 2785–2791 (2009).
- 15. Harris, R., Olson, A.J. & Goodsell, D.S. Automated prediction of ligand-binding sites in proteins. Proteins 70, 1506–1517 (2008).
- 16. Sousa, S.F. et al. Protein-ligand docking in the new millennium—a retrospective of 10 years in the field. *Curr. Med. Chem.* **20**, 2296–2314 (2013).
- 17. Goodsell, D.S., Lauble, H., Stout, C.D. & Olson, A.J. Automated docking in crystallography: analysis of the substrates of aconitase. Proteins 17, 1–10 (1993).
- 18. Goodsell, D.S., Morris, G.M. & Olson, A.J. Automated docking of flexible ligands: applications of AutoDock. *J. Mol. Recognit.* **9**, 1–5 (1996).
- 19. Soares, T.A., Goodsell, D.S., Briggs, J.M., Ferreira, R. & Olson, A.J. Docking of 4-oxalocrotonate tautomerase substrates: implications for the catalytic mechanism. Biolpolymers 50, 319–328 (1999).
- 20. Rosenfeld, R.J. et al. Automated docking of ligands to an artificial active site: augmenting crystallographic analysis with computer modeling. J. Comput. Aided Mol. Des. 17, 525–536 (2003).
- 21. Huey, R., Goodsell, D.S., Morris, G.M. & Olson, A.J. Grid-based hydrogen bond potentials in improved directionality. Lett. Drug Des. Discov. 1, 178–183 (2004).
- 22. Huey, R., Morris, G.M., Olson, A.J. & Goodsell, D.S. A semiempirical free energy force field with charge-based desolvation. J. Comput. Chem. 28, 1145–1152 (2006).
- 23. Forli, S. & Olson, A.J. A force field with discrete displaceable waters and desolvation entropy for hydrated ligand docking. J. Med. Chem. 55, 623–638 (2012).
- 24. Bianco, G., Forli, S., Goodsell, D.S. & Olson, A.J. Covalent docking using autodock: two-point attractor and flexible side chain methods. Protein Sci. 25, 295–301 (2016).
- 25. Cosconati, S. et al. Virtual screening with AutoDock: theory and practice. Expert Opin. Drug Discov. 5, 597–607 (2010).
- 26. Lin, J.H., Perryman, A.L., Schames, J.R. & McCammon, J.A. The relaxed complex method: accommodating receptor flexibility for drug design with an improved scoring scheme. Biopolymers 68, 47–62 (2003).